# Calibration Method for Measuring Structural Parameters of Few-mode Multi-core Fiber

Ziwen Liu[1], Jiajing Tu[1,*], Yongneng Jiang[1], Lei Shen[2], Lei Zhang[2], Liubo Yang[2], Weiping Liu[1], Zhaohui Li[3,4]

[1]Department of Electronic Engineering, College of Information Science and Technology, Jinan University, Guangzhou 510632, China
[2]State Key Laboratory of Optical Fiber and Cable Manufacture Technology, Yangtze Optical Fiber and Cable Joint Stock Limited Company, Wuhan 430073, China
[3]Guangdong Provincial Key Laboratory of Optoelectronic Information Processing Chips and Systems, Sun Yat-sen University, Guangzhou 510006, China
[4]Southern Laboratory of Ocean Science and Engineering, Guangdong, Zhuhai 519000, China
Corresponding author: tujiajing@jnu.edu.cn

***Abstract*—For the parameter measurement of the fabricated few-mode multi-core fibers (FM-MCFs), the accuracy cannot be guaranteed due to the power coupling among each core or each mode in these fibers. In this paper, using the sensitivity of the differential mode delay (DMD) and inter-core skew (ICS) to the relative refractive index difference between each layer and cladding, we compare the simulated DMD and ICS with the measured values to get the range of relative refractive index difference. Assisted by the image processing algorithm, the core diameter and core pitch of FM-MCF are also corrected. This correction method can give a more accurate parameter selection range for FM-MCF, so as to provide data support for FM-MCFs in transmission and sensing fields.**

***Keywords—FM-MCF, Image processing algorithm, DMD, ICS***

## I. INTRODUCTION

In recent years, the rapid growth of communication data traffic makes space division multiplexing (SDM) transmission technology have a broad application prospect in optical fiber communication system, and now SDM technology has received a lot of research attention. It may increase the system capacity by an order of magnitude [1]. Most research directions for SDM Fiber technology are multi-core fiber (MCF) and few-mode fiber (FMF) or a combination of the two [2]. The new FM-MCF which can realize super dense space division multiplexing (DSDM) is a reliable scheme to further increase the transmission channel and improve the transmission capacity [3-4].

Structural parameters such as core pitch, core diameter, and refractive index profile basically determine the optical performance of fiber. Therefore, it is particularly important to measure the optical parameters of the fiber before using the fiber. At present, the devices for measuring the refractive index profile of single-core single-mode fiber (SM-SCF) are relatively mature at home and abroad. For example, in 1979, interferometers began to be used for measuring the refractive index profile of SM-SCF. However, due to the use of interference patterns in this method, the measurement process is relatively complicated [5]. In 1981, Young proposed to use the refraction near-field method based on a refractometer to measure the refractive index profile of SM-SCF [6]. After cutting the fiber, the laser is incident from one end of the cut fiber segment, and the output power at the other end is received. With the cooperation of a lens which has a certain numerical aperture, matching liquid and photodetector, etc., the refractive index profile of the fiber is measured.

The above mentioned or other mature devices can be used to measure the parameters of SM-SCF. But for the SDM fiber, the existence of multiple cores causes coupling between cores, and the reduction of the core pitch increases the difficulty of designing measurement devices. At present, there is no mature device to measure the parameters of MCFs. Therefore, people design some methods to measure the parameters of MCF. Barty et al. proposed quantitative phase microscopy (QPM) method in 1998. They used a combination of quantitative phase-amplitude microscopy and tomographic reconstruction techniques for the simultaneous determination of three-dimensional absorption and refractive index distributions [7]. Through this method combined with computer technology, the core pitch, core diameter and refractive index profile of MCFs can be measured. In addition, reference [8] used the QPM method to avoid the damage caused by truncated optical fibers, and used the improved Brace-Köhler compensator (BKC) method to optimize the acquisition method of optical delay. Then they combined the machine vision technology to measure parameters of the single-mode seven-core fiber accurately. The accuracy of the relative refractive index difference is about $5\times10^{-4}$, and the errors of the core pitch and the core-clad radius position are about ±1.7μm and ±0.2μm, respectively. They provide a method for measuring the refractive index profile of the MCFs, and the accuracy is verified through experiments.

In this paper，we present another method to measure the parameters of FM-MCF. The core pitch and core diameter of the fiber are measured by image processing algorithm, and the errors are controlled at ±0.8μm and ±0.15μm, respectively. Furthermore, taking advantage of the sensitivity of DMD to relative refractive index difference and the sensitivity of ICS to bending and twist during fiber transmission [9,10], we modeled and simulated the fiber within the manufacturing error range of the design value given by YOFC to calculate the DMD and ICS of the fiber after long distance transmission. The range of relative refractive index difference can be obtained by comparing the simulated and measured values of DMD and ICS, and its precision is in the order of $1.6\times10^{-4}$. Through this method, more accurate parameters of FM-MCF are given.

## II. IMAGE PROCESSING

In 2014, Tu et al. proposed a relatively optimal design scheme for heterogeneous trench-assisted FM-MCF with low DMD and large effective area [11]. Based on this design scheme, we designed a homogeneous trench-assisted double-step seven-core three-mode fiber as shown in Fig. 1(a) to control DMD. This fiber mainly contains seven parameters, high refractive index core radius $a_1$, low refractive index core radius $r_1$, inner cladding radius $r_2$, trench radius $w$, high

relative refractive index difference $\Delta_1$, low relative refractive index difference $\Delta_2$, and trench relative refractive index difference $\Delta_t$. The fiber is manufactured by YOFC, and its manufacturing error range is shown in Table 1. The optical parameters of the fiber were corrected and compared with the values of the range.

TABLE I. MANUFACTURING ERROR RANGE

| | Units | Value | | Units | Value |
|---|---|---|---|---|---|
| $a_1$ | μm | 4.0±0.1 | $r_2$ | μm | 12.8±0.1 |
| $\Delta_1$ | % | 0.43±0.02 | $\Delta_t$ | % | -0.70±0.02 |
| $r_1$ | μm | 8.0±0.1 | $w_1$ | μm | 2.4±0.1 |
| $\Delta_2$ | % | 0.30±0.02 | $\Lambda$ | μm | 55.0±1.5 |

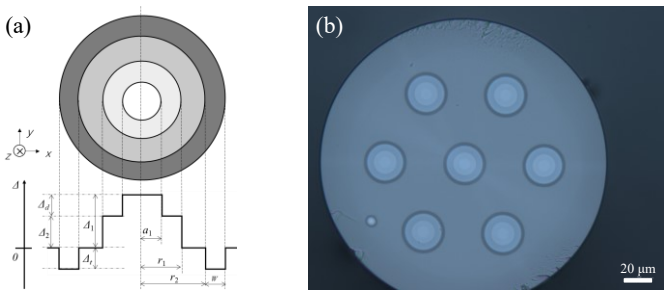


Fig. 1. (a). Designed refractive index profile, and, (b) microscope photograph of the homogeneous trench-assisted doubled-step seven-core three-mode fiber.

For this fiber, the microscope was used to photograph the optical fiber cross section as shown in Fig. 1(b). It is observed from the photograph that there is a marker to distinguish the different cores of the multi-core fiber. Due to the limitation of microscope measurement accuracy, there will be an error for the core diameter and core pitch measurement by a microscope. In reference [12], several photograph samples are processed by algorithms, and the core diameter is obtained by averaging the sample results. Therefore, we intercepted 16 samples of this fiber. The obtained 16 image samples were processed according to the image processing algorithm in Fig. 2. Firstly, the images captured by the microscope were processed by gray level binarization. Then, in order to obtain a clearer gray level histogram, the binarization images were further enhanced for contrast. Then the color of the image is differentiated by multi-threshold segmentation method.

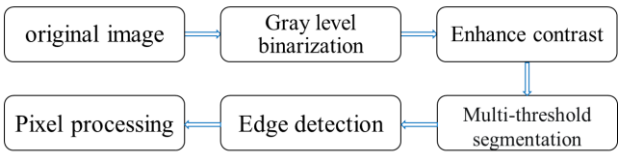


Fig. 2. Image processing algorithm.

One of the image samples split by the threshold is shown in Fig. 3(a). We calibrated the number of each core according to the position of the marker, so that different cores can be distinguished in subsequent experiments. Edge detection was carried out on Fig. 3(a), and each color zone was separated by a solid line, so the original fiber image was restored as shown in Fig. 3(b). For selecting more edge point values to restore the circle, we chose to use the least square method fitting the pixel points. Finally, the core diameter of each core was obtained respectively. Taking core 1 as an example, the core diameters obtained after image processing were $a_1$ = 4.0767μm, $r_1$ = 8.0805μm, $r_2$ = 12.9503μm, $w$ = 2.3231μm, and the core pitch between core 1 and core 2 was 55.7μm. The seven cores were all measured in this way, the error of the overall core diameter is within ± 0.15μm, and the error of the core pitch is within ±0.8μm.

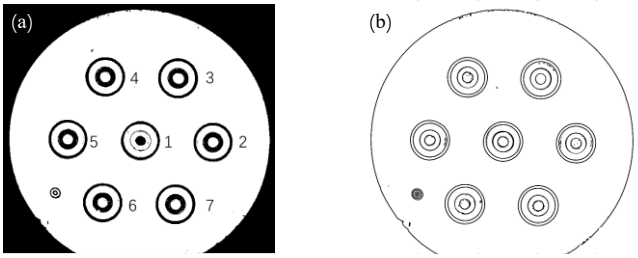


Fig. 3. (a). Threshold segmentation image, and, (b). edge detection image.

## III. EXPERIMENTAL MEASUREMENT SYSTEM

According to the experimental setup shown in Fig. 4, the time of flight (TOF) [13-14] method is used to measure the DMD of inter-mode and ICS between cores after 41 km transmission. Firstly, we used a tunable laser to emit a light source, and a digital-to-analog converter (DAC) input a low-frequency pulse to an electro-optical modulator (EMO). The optical path was collimated by a collimator (FC1), and the corresponding order mode was excited by a vortex phase plates (VPP). The generated beam which was focused by a 20×objective lens (20×OJ.) was coupled into the FM-MCF. The output beam from the corresponding core of FM-MCF was coupled with a multi-mode fiber (MMF) by the fusion splicer (FS). The SMF in the Fig. 4 is a reference single-mode fiber, and the waveform displayed in the oscilloscope (OSC) through this fiber corresponds to the reference waveform.

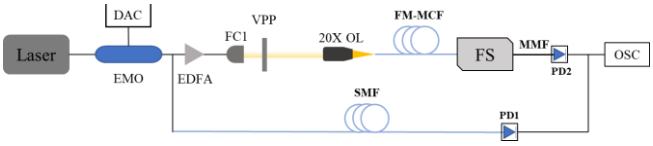


Fig. 4. TOF system: Laser: Tunable Laser, DAC: Digital-to-Analog Converter, EMO: Electro-optical modulator, EDFA: Erbium-doped fiber Amplifier, FC1: collimator, VPP: vortex phase plates, 20×OL: 20×Objective lens, FS: fusion splicer, PD: photo detector, OSC: oscilloscope.

Fig. 5(a) and Fig. 5(b) show the measurement results corresponding to core 1 and core 2 in Fig. 3(a). Taking core 1 and core 2 as examples, the DMD between $LP_{01}$ and $LP_{11}$ of core 1 is 9.6ns, and the delay of $LP_{01}$ mode in core 1 is 552ns based on the reference waveform, while the delay of $LP_{01}$ mode in core 2 is 534ns. Comparing the delay of the two cores, the ICS of $LP_{01}$ between core 1 and core 2 is 18ns. The other cores were measured in the same way, and the DMDs of cores 2-7 are 13ns, 7ns, 11ns, 12ns, 10ns, and 10ns respectively, and the ICS between cores 3-7 and core 1 were -1ns, 2ns, 14ns, 0ns, and 11ns, respectively.

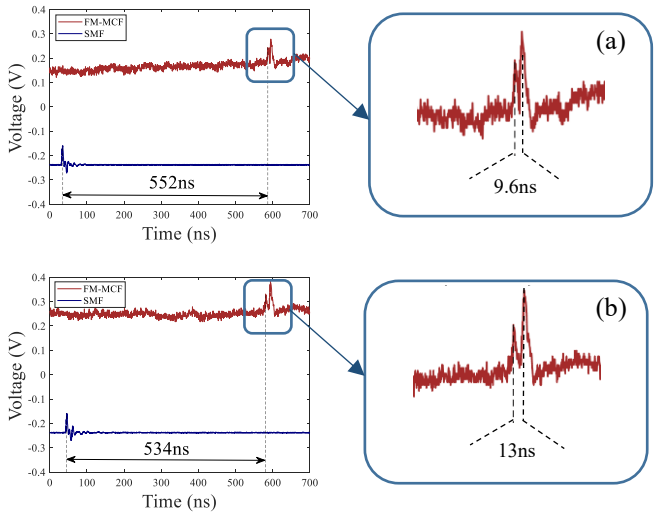


Fig. 5. (a). The measurement of DMD and delay of $LP_{01}$ for core1, and, (b). the measurement of DMD and delay of $LP_{01}$ for core2.

## IV. THEORETICAL SIMULATION

Based on the parameter values obtained by the image processing algorithm, the simulation of 41 km fiber within the manufacturing error range is carried out to obtain the simulated DMD and ICS.

### A. COMSOL modeling

Firstly, we used COMSOL to calculate the effective refractive index (*neff*) within the range of manufacturing error. It should be noted that, we did not add any bending and twisting when modeling. The $\Delta_t$ did not have much influence on the DMD and ICS, so only the corrections of $\Delta_1$ and $\Delta_2$ of this fiber are considered in this paper. Based on COMSOL, we modeled all the actual fibers and obtain the $neff_m$ of the core $m$ within the manufacturing error of $\Delta_1$ and $\Delta_2$.

### B. Simulation of bending and twisting fiber based on MATLAB

According to the segmentation theory [16] and the definition of DMD [17], a whole 41 km fiber is divided into $M$ short segments, each of which had a length of $\Delta L$. The difference mode transmission delay value after adding bending radius or twisting is calculated in each short segment. Finally, all delay values are superimposed to obtain the delay of the whole 41 km fiber. The time delay is calculated by the following formula:

$$t_{i,m}^{k} = \frac{\Delta L}{c} \cdot (neff_{eq,i,m} - \lambda \cdot \frac{dneff_{eq,i,m}}{d\lambda}), \tag{1}$$

where $t_{i,m}^{k}$ represents the time delay value of $k$ mode for core $m$ in the $i$ th short fiber; $c$ is the speed of light in vacuum; $neff_{eq,i,m}$ showed the equivalent effective refractive index of the $i$ th short fiber of core $m$ relative to the previous one; $\lambda$ is the wavelength. Each short segment is regarded as a straight fiber through the equivalent approximation condition [15]. According to the uniform approximation under the condition of weak derivation [10]:

$$neff_{eq,i,m} = neff_m(1 + \frac{r_m}{R_b}\cos\theta_{i,m}), \tag{2}$$

where $R_b$ represents the bending radius of the fiber; ($r_m$, $\theta_{i,m}$) is the local polar coordinate of core $m$; the size of $\theta_{i,m}$ is equal to the sum of twist value and $\theta_{i-1,m}$. Twist represents the sum of fixed and random twisting of the fiber. Fixed twist value is the bidirectional twisting added to reduce PMD when the fiber is rewired [18], and the random twist is the normal distribution random function *normrnd* added in the simulation process. Twist can be expressed by the (3):

$$\begin{aligned} twist = {} & AM \cdot \sin(i \cdot \Delta L \cdot \frac{2\pi}{T} + \frac{\pi}{2}) \cdot \Delta L \\ & + normrnd(mean, variance) \cdot \Delta L, \end{aligned} \tag{3}$$

where $AM$ and $T$ represented the amplitude and period of bidirectional twisting respectively; and the empirical value in the YOFC article were $AM = 30$ turn/m, $T = 1$ m [18]. *normrnd* with *mean* = 0 turn/m and *variance* = 0.0001 was used to generate a random number. The *mean* and *variance* were selected according to the changing trend of bending and twisting in DMD and ICS. We got the total delay after adding all short segments delay of $LP_{01}$ mode in (1).

As shown in Fig. 6(a) and 6(b), the horizontal axis represents $\Delta_1$ within the manufacturing error, and the vertical axis represents $\Delta_2$ within the manufacturing error. The dotted line in Fig. 6(a) and 6(b) represent the original design value. The solid line is the actual DMD of core 1 measured in experimental measurement system. Fig. 6(a) shows the DMD of core 1 within the manufacturing error after bending and twisting of 41 km fiber, and Fig. 6(b) shows the DMD of core 2 after bending and twisting of 41 km fiber within the manufacturing error.

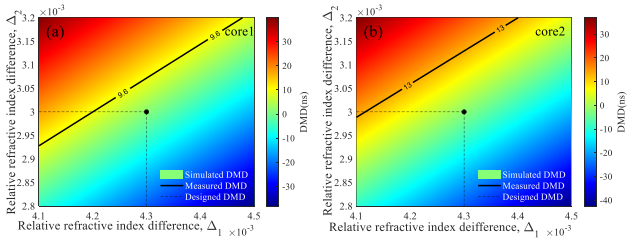


Fig. 6. (a) Measured and simulated DMD of core 1 within the manufacturing error of $\Delta_1$ and $\Delta_2$, and, (b) measured and simulated DMD of core 2 within the manufacturing error of $\Delta_1$ and $\Delta_2$.

### C. Comparison of simulated DMD, ICS and measured DMD, ICS

Taking core 1 and core 2 as the reference, in Fig. 6(a), the time delay of the fiber corresponding to the measured DMD of core 1 ($\Delta_1$ and $\Delta_2$ corresponding to the solid line in Fig. 6(a)) is subtracted from all the time delays obtained by core 2 in Fig. 6(b).

In the same way, all the time delay values of core 3-7 are subtracted from all time delays on the solid line in Fig. 6(a) to obtain the ICS between core 3-7 and core 1. By comparing the simulated and measured ICS, for example, Fig.7(a), (b), and (c) can be obtained. Comparing each figure in Fig. 7 with Fig. 6(b), the DMD of core 2 remains unchanged, while the white solid line which is labeled 18 represents the measured ICS between core 1 and core 2 by the experimental measurement system.

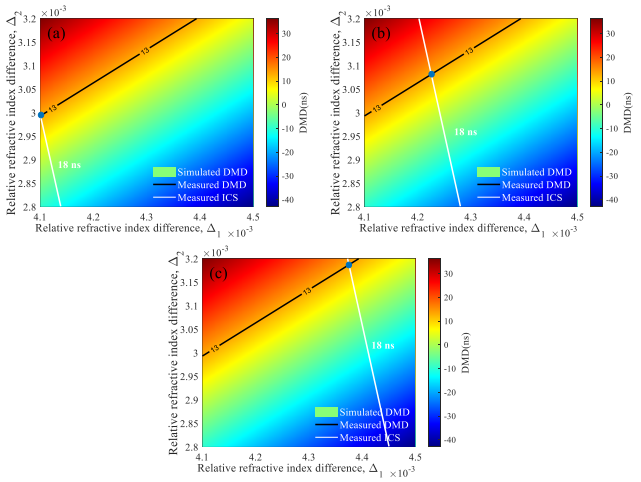


Fig. 7. The DMD of core 2 and the ICS between core 1 and core 2, (a). core1: $\Delta_1$ = 0.0042 and $\Delta_2$ = 0.00301, and, (b). core 1: $\Delta_1$ = 0.0043, $\Delta_2$=0.0031, and, (c). core 1: $\Delta_1$ = 0.00447, $\Delta_2$=0.0032.

Fig. 7(a) shows that when $\Delta_1$ = 0.0042 and $\Delta_2$ = 0.00301 of core 1, the figure of core 2 find one point which not only satisfy the measured DMD of core 2, but also satisfy the ICS of $LP_{01}$ between core 1 and core 2. The solid blue point in Fig. 7(a) is that point, which coordinate is (0.0041,0.003). That means when $\Delta_1$ = 0.0041 and $\Delta_2$ = 0.003 of core 2, $\Delta_1$ = 0.0042 and $\Delta_2$ = 0.00301 of core 1, the DMD of core 1 and core 2 satisfy the measured value and ICS between core 1 and core 2 is also equal to 18ns. If $\Delta_1$ and $\Delta_2$ of core 1 keep increasing, there will still have $\Delta_1$ and $\Delta_2$ of core 2 like the point in Fig. 7(a) that meets DMD and ICS of core 1 and core 2, as shown in Fig. 7(b). When $\Delta_1$ of core 1 increases to 0.00447 and $\Delta_2$ increase to 0.0032, the point also could find in the Fig. 7(c). However, if $\Delta_1$ and $\Delta_2$ of core 1 continues to increase, it will not have the fit value of the core 1 DMD. By comparing the DMD of core 1 with the DMD of core 2 and the ICS between them. Then the $\Delta_1$ of core 1 can be obtained in the range of 0.0042-0.00447, $\Delta_2$ in the range of 0.00301-0.0032, while the $\Delta_1$ of core 2 is in the range of 0.0041-0.004376, $\Delta_2$ ranges from 0.003-0.00319. In the same way, the $\Delta_1$ and $\Delta_2$ of the core 1 can be obtained by comparing core 1 with other cores respectively, and the corresponding value range of other cores can also be obtained. Finally, the relative refractive index error of each core can be obtained within $1.6\times10^{-4}$.

## V. Conclusion

In this paper, we propose a parameter measurement method for FM-MCF. The image processing algorithm is used to optimize the core diameter and core pitch of FM-MCF. The transmission of FM-MCF in bending and twisting state is simulated, and the measured values of DMD and ICS are compared with the simulated values to obtain the relative refractive index difference range. Through this method, we measured the parameters of a 41 km FM-MCF. Within the manufacturing error of parameters, the final relative refractive difference error is about $1.6\times10^{-4}$, and the errors of core pitch and core diameter are about ±0.8μm and ±0.15μm, respectively.

## Acknowledgment

This research was sponsored by Key Technologies Research and Development Program (2021YFB2800901); National Natural Science Foundation of China (U2001601); Guangzhou basic and applied basic research foundation (202002030327); Innovation Group Project of Southern Marine Science and Engineering Guangdong Laboratory (Zhuhai) (SML2022007); Key R&D Program of Hubei Province (Grants No. 2020BAB002); Guangdong Basic and Applied Basic Research Foundation No. 2023A1515012984.

## References

[1] B. Puttnam, G. Rademacher, and R. Luís, "Space-division multiplexing for optical fiber communications", Optica, vol. 8(9), pp. 1186-1203 2021.

[2] S. Gao, Y. Liu, R. Chen, and G. H, “Study on mode multiplexing used in space-division multiplexing”, Laser&Infrared, vol. 44 , pp. 424-428, 2014.

[3] J. Tu and Z. Li, “Review of Space Division Multiplexing Fibers”, Acta Optica Sinica, vol. 41(1), 0106003, 2021.

[4] K. Takenaga, Y. Sasaki, N. Guan, S. Matsuo, M. Kasahara, K. Saitoh, and M. Koshiba, “Large effective-area few-mode multicore fiber”, IEEE Photonics Technology Letters,vol. 24(21), pp. 1941-1944, 2012.

[5] H.M. Presby, D. Marcuse, H.W. Astle, and L.M. Boggs, “Rapid Automatic Index Profiling of Whole-Fiber Samples: Part II” Bell System Technical Journal, vol. 58(4), pp. 883-902, 1979.

[6] M. Young, “Optical fiber index profiles by the refracted-ray method (refracted near-field scanning)”, Applied Optics, vol. 20(19), pp. 3415-3422, 1981.

[7] A. Barty, K. A. Nugent, A. Roberts and D. Paganin, “Quantitative phase tomography”, Optics Communications, vol. 175(4-6), pp. 329-336, 2000.

[8] Y. Xie, L. Pei, Q. He, Y. Chang, Z. Guo, J, Wang, et al. “Reconstruction technology of refractive index and internal stress distribution of multi-core fibers (Invited)”, Laser&Infrared, vol. 51(1), 20210758, 2022.

[9] T. Mori, T. Sakamoto, M. Wada, T. Yamamoto and F. Yamamoto, "Few-mode fibers supporting more than two LP modes for mode-division-multiplexed transmission with MIMO DSP", Journal of Lightwave Technology, vol. 32(14), pp. 2468-2479. 2014.

[10] S. García, M. Urena, I. Gasulla, “Bending and twisting effects on multicore fiber differential group delay”, Optics express, vol. 27(22), pp. 31290-31298, 2019.

[11] J. Tu, S. Kunimasa, T. Katsuhiro, and M. Shoichiro, “Heterogeneous trench-assisted few-mode multi-core fiber with low differential mode delay”, Optics Express, vol. 22(4), pp. 4329-4341, 2014.

[12] L. Chen, J, Chen and R. Lu, “Optical fiber geometric parameter automatic detector”, Acta Optica Sinica, vol. 21(10), pp. 0253-2239, 2001.

[13] L. Cohen, "Comparison of single-mode fiber dispersion measurement techniques", Journal of lightwave technology vol. 3(5) pp. 958-966, 1985.

[14] J. Wiesenfeld and J. Stone, “Measurement of dispersion using short lengths of an optical fiber and picosecond pulses from semiconductor film laser”, Journal of lightwave technology, vol. 2(4), pp. 464-468, 1984.

[15] D. Marcuse, “Influence of curvature on the losses of doubly clad fibers”, Applied optics, vol. 21(23), pp. 4208-4213, 1982.

[16] B. Shemirani, M. Wei, A. Rahul Panicker and K. Joseph, “Principal modes in graded-index multimode fiber in presence of spatial-and polarization-mode coupling”, Journal of lightwave technology, vol. 27(10): pp. 1248-1261, 2009.

[17] J. Tu, S. Kunimasa, T. Katsuhiro and M. Shoichiro, “Heterogeneous trench-assisted few-mode multi-core fiber with low differential mode delay”, Optics Express, vol. 22(4), pp. 4329-4341, 2014.

[18] R. Wang and X. Jiang, “Fiber Spinning Technique for Improving PMD of the Fiber”, Optical Fiber &Electric Cable, vol. 3, pp. 1006-1908, 2006